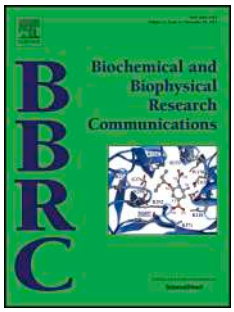

Apis mellifera RidA, a novel member of the canonical YigF/YER057c/UK114 imine deiminase superfamily of enzymes pre-empting metabolic damage

Cristina Visentin, Giulia Rizzi, Genny Degani, Stefania Digiovanni, Giovanni Robecchi, Alberto Barbiroli, Laura Popolo, Maria Antonietta Vanoni, Stefano Ricagno

PII: S0006-291X(22)00767-7

DOI: https://doi.org/10.1016/j.bbrc.2022.05.062

Reference: YBBRC 47453

To appear in: *Biochemical and Biophysical Research Communications*

Received Date: 6 May 2022

Accepted Date: 17 May 2022

Please cite this article as: C. Visentin, G. Rizzi, G. Degani, S. Digiovanni, G. Robecchi, A. Barbiroli, L. Popolo, M.A. Vanoni, S. Ricagno, *Apis mellifera* RidA, a novel member of the canonical YigF/YER057c/UK114 imine deiminase superfamily of enzymes pre-empting metabolic damage, *Biochemical and Biophysical Research Communications* (2022), doi: https://doi.org/10.1016/j.bbrc.2022.05.062.

Apis mellifera RidA, a novel member of the canonical YigF/YER057c/UK114 imine deiminase superfamily of enzymes pre-empting metabolic damage

Cristina Visentin[a,b], Giulia Rizzi[a], Genny Degani[a], Stefania Digiovanni[a], Giovanni Robecchi[a], Alberto Barbiroli[c], Laura Popolo[a], Maria Antonietta Vanoni[a], Stefano Ricagno[a,b*]

[a]Dipartimento di Bioscienze, Università degli Studi di Milano, via Celoria, 26, 20133, Milan, Italy

[b]Institute of Molecular and Translational Cardiology, I.R.C.C.S. Policlinico San Donato, piazza Malan, 2, 20097, San Donato Milanese, Italy

[c]Dipartimento di Scienze per gli Alimenti, la Nutrizione e l'Ambiente (DeFENS), Università degli Studi di Milano, via Celoria, 2, 20133, Milan, Italy

* Correspondence to: Stefano.ricagno@unimi.it

ABSTRACT

The Reactive intermediate deaminase (Rid) protein family is a group of enzymes widely distributed in all Kingdoms of Life. RidA is one of the eight known Rid subfamilies, and its members act by preventing the accumulation of 2-aminoacrylate, a highly reactive enamine generated during the metabolism of some amino acids, by hydrolyzing the 2-iminopyruvate tautomer to pyruvate and ammonia. RidA members are homotrimers exhibiting a remarkable thermal stability. Recently, a novel subclass of RidA was identified in teleosts, which differs for stability and substrate specificity from the canonical RidA. In this study we structurally and functionally characterized RidA from *Apis mellifera* ($_{Am}$RidA) as the first example of an invertebrate RidA to assess its belonging to the canonical RidA group, and to further correlate structural and functional features of this novel enzyme class. Circular dichroism revealed a spectrum typical of the RidA proteins and the high thermal stability. $_{Am}$RidA exhibits the 2-imino acid hydrolyze activity typical of RidA family members with a substrate specificity similar to that of the canonical RidA. The crystal structure confirmed the homotrimeric assembly and confirmed the presence of the typical structural features of RidA proteins, such as the proposed substrate recognition loop, and the ß-sheets ß1-ß9 and ß1-ß2. In conclusion, our data define $_{Am}$RidA as a canonical member of the well-conserved RidA family and further clarify the diagnostic structural features of this class of enzymes.

KEYWORDS

Imino acid deiminase, protein stability, metabolic damage, protein structure, RidA enzyme, substrate specificity.

INTRODUCTION

Reactive intermediate deaminase A (RidA) proteins are one of the eight groups of the large Rid (formerly YigF/YER057c/UK114) protein family and, differently from Rid1-7, are present in all domains of life [1–3]. These enzymes are crucial for metabolic homeostasis by removing intermediates responsible for cellular damage, primarily for their deaminase activity [4,5]. In particular, RidA is important to prevent 2-aminoacrylate (2AA) accumulation in cells. 2AA is produced by serine/threonine dehydratase and by cysteine desulfhydrase (Fig. S1). Its accumulation results in reduced cell fitness and alteration of metabolic pathways [1,6]. The exact mechanism of 2AA toxicity is still poorly understood, but it has been proposed that it may irreversibly inactivate pyridoxal-5′-phosphate-dependent enzymes and as yet unknown enzymes directly or through its stable 2-iminopyruvate (2IP) tautomer [7]. However, the variety of phenotypes observed for RidA mutants in different species suggests that RidA may function to prevent metabolic damage caused by reactive species other than 2AA/2IP.

The first mammalian RidA was extracted under native conditions from a perchloric acid-soluble fraction from *Capra hircus* (goat) liver ($_{Ch}$RidA), and it was initially investigated for its immunomodulatory activity against tumors [8]. Later, *in vitro* studies of the recombinant protein revealed its extraordinary thermal stability, and explored, on a quantitative basis, the catalytic efficiency of the enzyme with the respect to the hydrolysis of 2-imino acids (2IA) other than 2IP providing reference values. While the enzyme exhibits the highest catalytic efficiency with 2IP, *i.e.*, the only known physiological substrate, it can only hydrolyze to different extents 2IA carrying neutral and polar side chains, end even aromatic groups [9] suggesting that, indeed, RidA may protect cells from toxicity due to 2IA, other than 2IP, which may form in the cell.

All known RidA members share a homotrimeric fold. Three identical monomers possess a chorismate synthase-like fold and are assembled in a barrel-like structure with a central cavity

delimitated by the ß-sheets, and the α-helices exposed to the solvent. The active site lays at the interface between two adjacent monomers [10–18].

RidA is usually present as a single copy gene, except for *Saccharomyces cerevisiae* and teleost fishes [19,10]. In the bony fish *Salmo salar*, the two RidA isoforms ($_{Ss}$RidA1 and $_{Ss}$RidA2) exhibit a different substrate specificity and conformational stability, which can be correlated with a specific set of structural differences [10]. Interestingly, the comparison of such isoforms revealed the existence of a novel sub-class of RidA. Indeed, while $_{Ss}$RidA1 displays biochemical properties typical of canonical RidA family members, as exemplified by $_{Ch}$RidA, some properties were specific for $_{Ss}$RidA2. Compared to previously characterized RidA orthologues, $_{Ss}$RidA2 shows a generally lower catalytic efficiency with imino acids carrying neutral and polar side chains (including 2IP), but a marked activity with 2IA derived from aromatic amino acid and, unique among characterized RidA, from L-Glu. Furthermore, it unfolds at a significantly lower temperature compared to other RidA members [10]. All these differences could be explained by the structural analysis of the two salmon RidAs. Different inter- and intra-monomeric secondary structure interactions have been proposed to define the different conformational stability of the two salmon RidA and opposite conformations of the loop facing the catalytic site are responsible for distinct substrate specificity [10].

To clarify the molecular features that characterize canonical RidA, exemplified by $_{Ch}$RidA and $_{Ss}$RidA1, as opposed to the sub-class defined by $_{Ss}$RidA2, we selected the RidA from *Apis mellifera*, as model RidA from invertebrates, and we report its biochemical and structural characterization.

MATERIAL AND METHODS

$_{Am}$RidA protein expression and purification

To identify invertebrate RidAs we carried out a BLASTP similarity search, applying default parameters, in the entire protein database using the human RidA ($_{Hs}$RidA, 136 amino acids). Two putative proteins (XP_003251902_3 and XP_016772925_2) were identified in *Apis mellifera*, the former of 137 amino acids ($_{Am}$RidA) shares 50% identity with $_{Hs}$RidA and the latter of 114 residues ($_{Am}$RidA-v1) lacks residues from 78 to 101 and likely originated from the skipping of the fourth exon during *ridA* transcript maturation. In *Apis florea*, the same two forms were detected suggesting the existence of a single copy *ridA* gene and a common pattern of alternative splicing in *Apis* genera. The $_{Am}$RidA and $_{Am}$RidA-v1 DNA coding sequences were codon optimized for expression in *E. coli*, synthetized by GENEWIZ GmbH (Leipzig, Germany) and cloned into a pET15b expression vector (Novagen) between *NdeI* and *XhoI* restriction sites. The fusion recombinant protein carries N-terminal 6XHis-tag and thrombin protease recognition sequence. $_{Am}$RidA and $_{Am}$RidA-v1 were overexpressed and purified in Rosetta(DE3)pLysS *E. coli* cells as described in Degani *et al.* [9]. Both proteins were produced but $_{Am}$RidA-v1 was insoluble and no further work was done on it.

Analytical size exclusion

Superdex 75 Increase 10/300 GL (GE Healthcare, USA) column equilibrated with 154 mM NaCl, which had been previously calibrated with proteins of known molecular mass, was used to analyze an aliquot of $_{Am}$Rid.

Circular dichroism

Circular dichroism (CD) spectroscopy and CD-monitored thermal denaturation were carried out as described in Digiovanni *et al.* [10]. The melting temperature (T_m) values were calculated as the first-derivative minimum of the traces.

Protein sequences comparison

$_{Am}$RidA (UniProt KB: A0A7M7GBQ0), $_{Ch}$RidA (UniProt KB: P80601), $_{Ss}$RidA1 (UniProt KB: A0A1S3KNQ3) and $_{Ss}$RidA2 (UniProt KB: C0H8I4) sequences were aligned using

ClustalOmega [20]. Protein alignment was then analyzed and visualized by ESPript 3.0[21]. Sequences were also compared using BLAST-P [22].

RidA activity assay

Activity assays were carried out as detailed in Digiovanni *et al*. [23]. Since 2IA are unstable species undergoing spontaneous hydrolysis, they must be generated *in situ* by the action of an amino acid oxidase in the presence of a given amino acid. Semicarbazide is included in the assay in order to monitor the generation of the 2IA spectrophotometrically at 248 nm as the spontaneous formation of the corresponding semicarbazone. Thus, 150 µl reaction mixtures containing 5 mM semicarbazide, 1 µg catalase, varying RidA concentrations, and an amount of commercial L-amino acid oxidase able to generate the 2IA at an initial rate yielding 0.2-0.4 ΔA_{248}/min in the absence of RidA, in 50 mM sodium pyrophosphate buffer, pH 8.7, were equilibrated at 25 °C. The reaction was started by adding the L-amino acid solution at a 5 mM final concentration. To assay for activity with 2-iminoglutarate, L-glutamate oxidase was used with L-Glu. Due to the high absorption of L-Trp in the UV region, its concentration was lowered to 0.5 mM. The values of the percental residual initial velocity (v, %) measured in the presence of varying RidA concentration with respect to that measured in the absence of RidA are fitted with Eq 1 where K_{50} is the concentration of RidA that halves the initial velocity of the reaction observed in the absence of RidA. It has been shown [9] that $100/K_{50}$ is an estimate of the catalytic efficiency of RidA (k_{cat}/K_m) with the given 2IA. Given the type of coupled assay, no information on individual values of k_{cat} and K_m values can be obtained. In the presence of 2IA that are poor substrates of RidA, the v, % values obtained at varying RidA can be fitted to a straight line. Its slope provides the $100/K_{50}$ value [9]. The indole pyruvate product of the hydrolysis of the 2IA produced from L-Trp exhibits detectable absorbance at 248 nm leading to a non-zero value of the reaction velocity at high RidA concentrations. Thus, residual

activity values (v, %) as a function of RidA concentration were fitted to Eq 2, in which *C* is the constant v, % value reached at infinite RidA concentration.

Eq 1 $$v, \% = \frac{100}{1+\frac{[RidA]}{K50}}$$

Eq 2 $$v, \% = \frac{100-C}{1+\frac{[RidA]}{K50}} + C$$

Protein crystallization and structure determination

Purified $_{Am}$RidA (9 mg/ml) in 154 mM NaCl was subjected to crystallization trials using an Oryx4 crystallization robot (Douglas Instruments, UK). Crystallization screening experiments were performed in sitting drop and crystallization plates were incubated at 20 °C. Single crystals suitable for X-ray diffraction experiments grew overnight from PACT screen (Molecular dimensions, USA) condition B10. Crystals were cryo-protected adding 25% glycerol and flash-frozen in liquid nitrogen.

X-ray diffraction data were collected at cryogenic temperature (100 K) at the European Synchrotron Radiation Facility (ESRF, Grenoble, France) on ID23-1 beamline equipped with a Pilatus 6M (Dectris) detector.

$_{Am}$RidA structure was determined by molecular replacement by MOLREP [24] using the coordinates of the human hp14.5 protein (PDB: 1ONI) as search model. Initial molecular replacement solutions were subjected to subsequent cycles of manual building in Coot [25] and refinement with phenix.refine [26]. Models were inspected and validated using Molprobity [27]; processing and refinement statistics are reported in Table S1. Coordinates and structure factors have been deposited in the PDB under the accession code 7ZS6. Structural images were generated using CCP4mg [28].

RESULTS AND DISCUSSION

$_{Am}$RidA purification, and characterisation

Recombinant $_{Am}$RidA was expressed in Rosetta(DE3)pLysS *E. coli* cells and purified to homogeneity as previously reported for goat and salmon RidAs [9,23]. To assess the oligomeric state of $_{Am}$RidA in solution, analytical size exclusion chromatography was performed. Purified $_{Am}$RidA eluted in a symmetric single peak at 14.7 ml, compatible with an apparent mass of 43.0 kDa (Fig. 1A), *i.e.*, a homotrimeric assembly (theoretical molecular mass 46.1 kDa) analogously to what observed for other RidA family members [9–14,16]. Far UV CD was then performed to investigate the secondary structure content. As reported in Figure 1B, $_{Am}$RidA showed a typical α/ß-spectrum with an estimated 41% of α-helixes and 39% of ß-sheets, well matching data reported for other RidA family members [9,10]. Then, to establish $_{Am}$RidA thermostability, molar ellipticity at 220 nm was monitored between 20 and 98 °C (Fig. 1C). The estimated T_m is 82 °C, in line with the stability previously reported for other canonical members of the RidA family ($_{Ch}$RidA: 104 °C and $_{Ss}$RidA-1: 100.2 °C) [9,10], whereas $_{Ss}$RidA2 has a T_m of 65 °C [10].

$_{Am}$RidA enzymatic activity

In order to evaluate $_{Am}$RidA enzymatic activity, the ability to hydrolyze selected 2IA was monitored using the previously established enzymatic assay [23]. Figure 2 shows that $_{Am}$RidA exhibits the same order of substrate preference as that previously reported for $_{Ch}$RidA and $_{Ss}$RidA1. As shown in Table 1 and Figure 2, it stands out among RidA members exhibiting the highest catalytic efficiency for 2IP, derived from L-Ala. The activity with L-Trp is also half of that of $_{Ch}$RidA, while it is poorly active with L-Phe and L-Glu derivatives and fully inactive with the 2IA derived from L-His like $_{Ch}$RidA and $_{Ss}$RidA1. Thus, the low activity with the derivatives of L-Ala and L-Leu compared to the activity with 2-iminoglutarate is confirmed to be distinctive feature of the novel non-canonical $_{Ss}$RidA2. On the other hand, the canonical RidA enzymes show the highest catalytic activity for 2IP, supporting the concept that it is the

physiological substrate of this class of enzymes. However, the ability to accept 2IA with hydrophobic or aromatic side chains like L-Leu and L-Trp derivatives suggests that it may also serve other (yet unknown) functions in the cell.

$_{Am}$RidA sequence analysis

The sequence of $_{Am}$RidA was aligned to those of $_{Ch}$RidA, $_{Ss}$RidA1 and $_{Ss}$RidA2 (Fig. 3A). This comparison is focused on the sequences of RidA proteins for which comparable biochemical and structural characterization is available [9,10,13]. $_{Am}$RidA shares high sequence identity with these RidA family members: most of the sequence variability is localized in the N-terminal stretch; indeed, after the 17 initial residues, the degree of identity is about 50% (Fig. 3A). The insect protein, compared to goat or salmon ones, exhibits an extension of 2 amino acids at the N-terminus. BLAST-P analysis reported a total score of alignment of 153, 150 and 142 when $_{Am}$RidA sequence was compared to $_{Ss}$RidA1, $_{Ch}$RidA and $_{Ss}$RidA2, respectively, with a query coverage of 91%, 94% or 89%, respectively. These data indicate that, even though the sequence identity is comparable among the proteins, $_{Am}$RidA homology is higher with $_{Ss}$RidA1 and $_{Ch}$RidA than with $_{Ss}$RidA2.

$_{Am}$RidA crystal structure determination

The crystal structure of $_{Am}$RidA was determined to 1.31 Å resolution. The homotrimeric assembly of $_{Am}$RidA was confirmed (Fig. 3B). Each monomer presents a chorismate mutase-like fold and consists of a six-stranded ß-sheet packed against two α-helices (Fig. 3C). Therefore, the typical fold of the RidA family is maintained [11–18,23,29]. The three active sites are at the interface between subunits with a geometry reminiscent of that of other RidA family members [12,16]. $_{Am}$RidA structure was compared to other RidA crystal structures available: $_{Ch}$RidA (PDB: 1NQ3) resulted in a r.m.s.d. of 0.77 over 398 Cα; $_{Ss}$RidA1 (PDB: 6TCC) with an r.m.s.d. of 0.82 over 400 Cα; and $_{Ss}$RidA2 (PDB: 6TCD) with r.m.s.d. value of 0.89 over 377 Cα. Thus, it is confirmed that RidA are overall structurally very similar.

However, inspection of the N-terminal regions provides valuable information on the structure-function relation. Indeed, compared to $_{Ss}$RidA1 and $_{Ch}$RidA, the non-canonical $_{Ss}$RidA2 displays specific local features that were proposed to correlate with thermal stability and substrate specificity of the enzymes [10]. The loop connecting ß-strand 1 and 2 and facing the catalytic residue Arg109 (Arg107 in goat and salmon RidA) has been proposed to be crucial for substrate recognition [10]. This loop in $_{Am}$RidA shows several differences compared to goat and salmon RidA: a Lys is present at position 18 in place of an Ala or Gly residue. Even though this is not a conservative substitution, the side chain of Lys18 is exposed to solvent and not toward the inner cavity, thus not affecting the chemical and steric properties of the active site. Moreover, a Pro in position 19 in place of an Ala does not affect the loop conformation, while Ile 20 is conservatively substituted to a Val (Fig. 3A and D). Crucially, the Pro17 that locks the loop in a specific conformation in $_{Ch}$RidA and $_{Ss}$RidA1 is conserved. Opposite to the salmon RidA structures, this loop displays two different conformations in the $_{Am}$RidA structure where Pro19 and Val20 side chains flip. This indicates the plasticity of this loop. However, the overall loop conformation and active site cavity are reminiscent of the ones observed in $_{Ch}$RidA and $_{Ss}$RidA1. The distinct geometry and the wealth of positive charges present in $_{Ss}$RidA2 recognition loop are not found in $_{Am}$RidA (Fig. 3E). Thus, these observations well explain the fact that $_{Am}$RidA substrate specificity is more comparable to that of $_{Ch}$RidA or $_{Ss}$RidA1, than to $_{Ss}$RidA2. The replacement of Ala15 of $_{Ch}$RidA and $_{Ss}$RidA1 with a Pro residue likely decreases the conformational flexibility of the loop and may explain the higher catalytic efficiency with 2IP of $_{Am}$RidA with respect to those of $_{Ch}$RidA and $_{Ss}$RidA1. Indeed, despite an overall conservation of general geometry, the cavity delimitating the active site of $_{Am}$RidA shows a reduced hydrophobicity compared to goat and salmon RidA, well matching with observed substrate preference.

A second compelling difference between $_{Ss}$RidA1 and $_{Ss}$RidA2 structures is the ß-structure content: compared to $_{Ss}$RidA2, $_{Ss}$RidA1 has an extended β2-strand, interacting with ß1-strand, and an additional C-terminal β9-strand which interacts with β1-strand of the adjacent monomer. The presence of such additional ß-interactions was suggested to account for the significantly higher thermal stability of $_{Ss}$RidA1 compared to $_{Ss}$RidA2 [10]. $_{Am}$RidA ß-sheets resemble the specific traits of $_{Ss}$RidA1. Indeed, the formation of ß-sheet between ß1-strand at the N-terminal region of a monomer and ß9-strand at the C-terminal of the neighboring subunit was observed (Fig. 3F). These ß-interactions contribute to $_{Am}$RidA protein stability.

Moreover, the extent of intra-monomeric ß-interactions between strands β1 and β2 may play a relevant role in determining protein stability. In $_{Am}$RidA β1 ranges from residue 7 to 11 and β2 from residue 26 to 30, analogously to what was observed in $_{Ss}$RidA1 and $_{Ch}$RidA (Fig. 3G). Conversely in $_{Ss}$RidA2 Pro11, instead of an Ile residue, shortens β1 and decreases its stabilization effect.

In conclusion, the structural and biochemical data presented in this work demonstrate that RidA from *Apis mellifera*, chosen as a model of invertebrate RidAs, is more closely related to the canonical members of the RidA family than with the non-canonical sub-class recently found in teleost. Therefore, the present study, beside demonstrating the presence of a RidA activity also in invertebrates, further clarifies the structural features that help defining the conformational stability and substrate specificity of RidA members.

AKNOWLEDGEMENTS

The work in SR laboratory was supported by Fondazione Baggi Sisini, and, in part, by Fondazione ARISLA (project TDP- 43-STRUCT), Fondazione Telethon (GGP17036) and by Ricerca Corrente funding from Italian Ministry of Health to IRCCS Policlinico San Donato.

Fondazione U. Veronesi is gratefully acknowledged for the support to CV. We kindly acknowledge Prof. A. Bartorelli and Prof. S. Minucci for helpful discussions.

BIBLIOGRAPHY

[1] T.D. Niehaus, S. Gerdes, K. Hodge-Hanson, A. Zhukov, A.J.L. Cooper, M. ElBadawi-Sidhu, O. Fiehn, D.M. Downs, A.D. Hanson, Genomic and experimental evidence for multiple metabolic functions in the RidA/YjgF/YER057c/UK114 (Rid) protein family, BMC Genomics. 16 (2015) 382. https://doi.org/10.1186/s12864-015-1584-3.

[2] K.M. Hodge-Hanson, D.M. Downs, Members of the Rid protein family have broad imine deaminase activity and can accelerate the Pseudomonas aeruginosa D-arginine dehydrogenase (DauA) reaction in vitro, PloS One. 12 (2017) e0185544. https://doi.org/10.1371/journal.pone.0185544.

[3] J.L. Irons, K. Hodge-Hanson, D.M. Downs, RidA Proteins Protect against Metabolic Damage by Reactive Intermediates, Microbiol. Mol. Biol. Rev. MMBR. 84 (2020) e00024-20. https://doi.org/10.1128/MMBR.00024-20.

[4] J.A. Lambrecht, G.E. Schmitz, D.M. Downs, RidA proteins prevent metabolic damage inflicted by PLP-dependent dehydratases in all domains of life, MBio. 4 (2013) e00033-00013. https://doi.org/10.1128/mBio.00033-13.

[5] D.M. Downs, D.C. Ernst, From microbiology to cancer biology: the Rid protein family prevents cellular damage caused by endogenously generated reactive nitrogen species, Mol. Microbiol. 96 (2015) 211–219. https://doi.org/10.1111/mmi.12945.

[6] A.J. Borchert, J.M. Walejko, A.L. Guennec, D.C. Ernst, A.S. Edison, D.M. Downs, Integrated Metabolomics and Transcriptomics Suggest the Global Metabolic Response to 2-Aminoacrylate Stress in Salmonella enterica, Metabolites. 10 (2019) E12. https://doi.org/10.3390/metabo10010012.

[7] A.J. Borchert, D.C. Ernst, D.M. Downs, Reactive Enamines and Imines In Vivo: Lessons from the RidA Paradigm, Trends Biochem. Sci. 44 (2019) 849–860. https://doi.org/10.1016/j.tibs.2019.04.011.

[8] A. Bartorelli, C. Biancardi, V. Cavalca, R. Ferrara, M. Botta, C. Arzani, I. Colombo, B. Berra, F. Ceciliani, S. Ronchi, M. Bailo, Purification and partial characterization of proteins present in a perchloric acid extract of goat liver (UK101), J. Tumor Marker Oncol. 11 (1996) 57–61.

[9] G. Degani, A. Barbiroli, L. Regazzoni, L. Popolo, M.A. Vanoni, Imine Deaminase Activity and Conformational Stability of UK114, the Mammalian Member of the Rid Protein Family Active in Amino Acid Metabolism, Int. J. Mol. Sci. 19 (2018) E945. https://doi.org/10.3390/ijms19040945.

[10] S. Digiovanni, C. Visentin, G. Degani, A. Barbiroli, M. Chiara, L. Regazzoni, F. Di Pisa, A.J. Borchert, D.M. Downs, S. Ricagno, M.A. Vanoni, L. Popolo, Two novel fish paralogs provide insights into the Rid family of imine deaminases active in pre-empting enamine/imine metabolic damage, Sci. Rep. 10 (2020) 10135. https://doi.org/10.1038/s41598-020-66663-w.

[11] S. Kwon, C.W. Lee, H.Y. Koh, H. Park, J.H. Lee, H.H. Park, Crystal structure of the reactive intermediate/imine deaminase A homolog from the Antarctic bacterium Psychrobacter sp. PAMC 21119, Biochem. Biophys. Res. Commun. 522 (2020) 585–591. https://doi.org/10.1016/j.bbrc.2019.11.139.

[12] X. Liu, J. Zeng, X. Chen, W. Xie, Crystal structures of RidA, an important enzyme for the prevention of toxic side products, Sci. Rep. 6 (2016) 30494. https://doi.org/10.1038/srep30494.
[13] D. Deriu, C. Briand, E. Mistiniene, V. Naktinis, M.G. Grütter, Structure and oligomeric state of the mammalian tumour-associated antigen UK114, Acta Crystallogr. D Biol. Crystallogr. 59 (2003) 1676–1678. https://doi.org/10.1107/s0907444903014306.
[14] B.A. Manjasetty, H. Delbrück, D.-T. Pham, U. Mueller, M. Fieber-Erdmann, C. Scheich, V. Sievert, K. Büssow, F.H. Niesen, W. Weihofen, B. Loll, W. Saenger, U. Heinemann, F.H. Neisen, Crystal structure of Homo sapiens protein hp14.5, Proteins. 54 (2004) 797–800. https://doi.org/10.1002/prot.10619.
[15] H. Zhang, Y. Gao, M. Li, W. Chang, Crystal structure of the PSPTO-PSP protein from Pseudomonas syringae pv. tomato str. DC3000 in complex with D-glucose, Biochem. Biophys. Res. Commun. 397 (2010) 82–86. https://doi.org/10.1016/j.bbrc.2010.05.071.
[16] J.D. Burman, C.E.M. Stevenson, R.G. Sawers, D.M. Lawson, The crystal structure of Escherichia coli TdcF, a member of the highly conserved YjgF/YER057c/UK114 family, BMC Struct. Biol. 7 (2007) 30. https://doi.org/10.1186/1472-6807-7-30.
[17] A.M. Deaconescu, A. Roll-Mecak, J.B. Bonanno, S.E. Gerchman, H. Kycia, F.W. Studier, S.K. Burley, X-ray structure of Saccharomyces cerevisiae homologous mitochondrial matrix factor 1 (Hmf1), Proteins. 48 (2002) 431–436. https://doi.org/10.1002/prot.10151.
[18] T. Miyakawa, W.C. Lee, K. Hatano, Y. Kato, Y. Sawano, K. Miyazono, K. Nagata, M. Tanokura, Crystal structure of the YjgF/YER057c/UK114 family protein from the hyperthermophilic archaeon Sulfolobus tokodaii strain 7, Proteins. 62 (2006) 557–561. https://doi.org/10.1002/prot.20778.
[19] G.H. Whitaker, D.C. Ernst, D.M. Downs, Absence of MMF1 disrupts heme biosynthesis by targeting Hem1pin Saccharomyces cerevisiae, Yeast Chichester Engl. 38 (2021) 615–624. https://doi.org/10.1002/yea.3670.
[20] F. Madeira, Y.M. Park, J. Lee, N. Buso, T. Gur, N. Madhusoodanan, P. Basutkar, A.R.N. Tivey, S.C. Potter, R.D. Finn, R. Lopez, The EMBL-EBI search and sequence analysis tools APIs in 2019, Nucleic Acids Res. 47 (2019) W636–W641. https://doi.org/10.1093/nar/gkz268.
[21] X. Robert, P. Gouet, Deciphering key features in protein structures with the new ENDscript server, Nucleic Acids Res. 42 (2014) W320–W324. https://doi.org/10.1093/nar/gku316.
[22] S.F. Altschul, T.L. Madden, A.A. Schäffer, J. Zhang, Z. Zhang, W. Miller, D.J. Lipman, Gapped BLAST and PSI-BLAST: a new generation of protein database search programs, Nucleic Acids Res. 25 (1997) 3389–3402. https://doi.org/10.1093/nar/25.17.3389.
[23] S. Digiovanni, G. Degani, L. Popolo, M.A. Vanoni, Using d- and l-Amino Acid Oxidases to Generate the Imino Acid Substrate to Measure the Activity of the Novel Rid (Enamine/Imine Deaminase) Class of Enzymes, in: M. Barile (Ed.), Flavins Flavoproteins Methods Protoc., Springer US, New York, NY, 2021: pp. 199–218. https://doi.org/10.1007/978-1-0716-1286-6_13.
[24] A. Vagin, A. Teplyakov, Molecular replacement with MOLREP, Acta Crystallogr. D Biol. Crystallogr. 66 (2010) 22–25. https://doi.org/10.1107/S0907444909042589.
[25] P. Emsley, K. Cowtan, Coot: model-building tools for molecular graphics, Acta Crystallogr. D Biol. Crystallogr. 60 (2004) 2126–2132. https://doi.org/10.1107/S0907444904019158.
[26] P.V. Afonine, R.W. Grosse-Kunstleve, N. Echols, J.J. Headd, N.W. Moriarty, M. Mustyakimov, T.C. Terwilliger, A. Urzhumtsev, P.H. Zwart, P.D. Adams, Towards

automated crystallographic structure refinement with phenix.refine, Acta Crystallogr. D Biol. Crystallogr. 68 (2012) 352–367. https://doi.org/10.1107/S0907444912001308.
[27] V.B. Chen, W.B. Arendall, J.J. Headd, D.A. Keedy, R.M. Immormino, G.J. Kapral, L.W. Murray, J.S. Richardson, D.C. Richardson, MolProbity: all-atom structure validation for macromolecular crystallography, Acta Crystallogr. D Biol. Crystallogr. 66 (2010) 12–21. https://doi.org/10.1107/S0907444909042073.
[28] S. McNicholas, E. Potterton, K.S. Wilson, M.E.M. Noble, Presenting your structures: the CCP4mg molecular-graphics software, Acta Crystallogr. D Biol. Crystallogr. 67 (2011) 386–394. https://doi.org/10.1107/S0907444911007281.
[29] J. Kim, R.A. Denu, B.A. Dollar, L.E. Escalante, J.P. Kuether, N.S. Callander, F. Asimakopoulos, P. Hematti, Macrophages and mesenchymal stromal cells support survival and proliferation of multiple myeloma cells, Br. J. Haematol. 158 (2012) 336–346. https://doi.org/10.1111/j.1365-2141.2012.09154.x.

FIGURE LEGENDS

Figure 1. $_{Am}$RidA characterization. (A) $_{Am}$RidA analytical size exclusion chromatography on a Superdex 75 10/300. (B) Far-UV CD spectrum of $_{Am}$RidA (0.2 mg/ml) recorded at 20 °C in 154 mM NaCl in a 0.1 cm path length cuvette. (C) CD-monitored thermal denaturation of $_{Am}$RidA while heating at 1°C/min.

Figure 2. Substrate specificity of $_{Am}$RidA. (A) The percental residual activity (v, %) measured at varying $_{Am}$RidA concentrations was calculated with reference to that measured in the absence of $_{Am}$RidA in assays containing L-Leu (empty circles), L-Ala (empty squares), L-Trp (empty triangles), L-Phe (inverse triangles), L-Glu (diamonds) or L-His (stars) as the L-amino acid oxidase substrate in 50 mM sodium pyrophosphate buffer, pH 8.7, as described in the Methods section. Curves are the best fit of the data to Eq 1 except for data obtained with L-Glu and L-Phe that were fitted to a straight line and those obtained with L-Trp that were fitted to Eq 2. No significant decrease of reaction velocity was obtained in the presence of the 2IA generated with the L-His/LAAO couple. The calculated K_{50} and $100/K_{50}$ values are in Table 1. (B) Catalytic efficiencies of $_{Ch}$RidA (blue), $_{Ss}$RidA1 (orange), $_{Ss}$RidA2 (grey) and $_{Am}$RidA (yellow) expressed as $100/K_{50}$ with respect to the hydrolysis of the IA derived *in situ* from the indicated L-amino acids upon reaction with L-amino acid oxidase. When no vertical bar is observed, no activity with the given imino acid was detected.

Figure 3. Comparison of $_{Am}$RidA to other canonical RidA proteins. (A) Primary structures of $_{Am}$RidA, $_{Ch}$RidA, $_{Ss}$RidA1 and $_{Ss}$RidA2 were aligned with ClustalOmega. The result of alignment was analyzed by ESPript3 software. Identical residues are represented in white lettering against a red background; similar residues are indicated in red and blue frames indicate sequence stretches with globally high similarity. (B-C) $_{Am}$RidA is an homotrimer (B) composed

of three monomers with a chorismate synthase-like fold (C). (D) Representation of the loop connecting ß1 and ß2 strands. (E) Structural superposition of the recognition loop of RidA from different species. (F-G) Stick representation of inter-monomeric ß-sheet formed between ß1 and ß9 strands of adjacent monomers (F) and of the intra-monomeric ß-sheet between ß1 and ß2 strands (G).

Table 1. Specificity of $_{Am}$RidA

Amino acid	$_{Ch}$RidA		$_{Ss}$RidA1[a]		$_{Ss}$RidA2a		$_{Am}$RidA	
	K_{50}, μM	$100/K_{50}$, μM^{-1}	K_{50}, μM	$100/K_{50}$, μM^{-1}	K_{50}, μM	$100/K_{50}$, μM^{-1}	K_{50}, μM	$100/K_{50}$, μM^{-1}
L-Leu	0.45±0.03[b]	222 ± 13	0.89±0.07[b]	112±9	52.6±4.2[b]	1.9±0.15	0.9±0.04[b]	109.6±4.3
L-Ala	0.29±0.02[b]	345±24	0.2±0.01[b]	489±23	2.6±0.15[b]	38.9±2.2	0.16±0.01[b]	628.5±33.6
L-His	52.6±27.7	1.9±1[c]	NA		102±10.4[b]	0.98±0.1[c]	NA	
L-Phe	40±3.2	2.5±0.2[c]	71.4±10.2[b]	1.4±0.2	11.5±1.2[a]	8.7±0.9	38.9±2.1	2.57±0.14[c]
L-Trp	0.98±0.12[d]	102±84	5.8±0.3[b]	17.2±0.9	5.75±0.5[b]	17.4±1.5	1.86±0.21[d]	53.7±6.0
L-Glu	10.9±0.3[b]	9.1±0.3	2.48±0.2[b]	40.4±3.3	0.48±0.06[b]	210±25	178.9±44.8	0.56±0.14[c]

NA, no activity detected. [a]Data from Di Giovanni *et al.* [10]. [b]Data fitted with Eq 1 that yields the K_{50} value from which $100/K_{50}$ is calculated. [c]Data were fitted to a straight line, the slope of which is $100/K_{50}$ from which K_{50} was calculated. [d]Data were fitted with Eq 2. C was 16.4 ± 2.8 for $_{Ch}$RidA and 15.2±3.1 for $_{Am}$RidA.

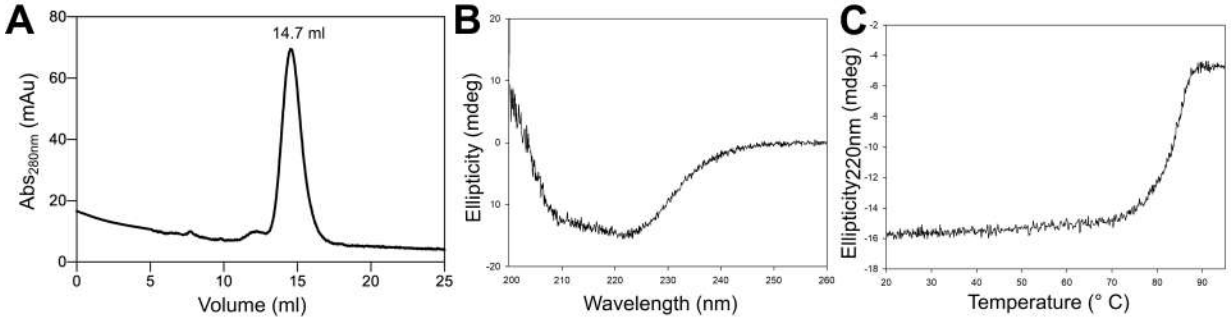

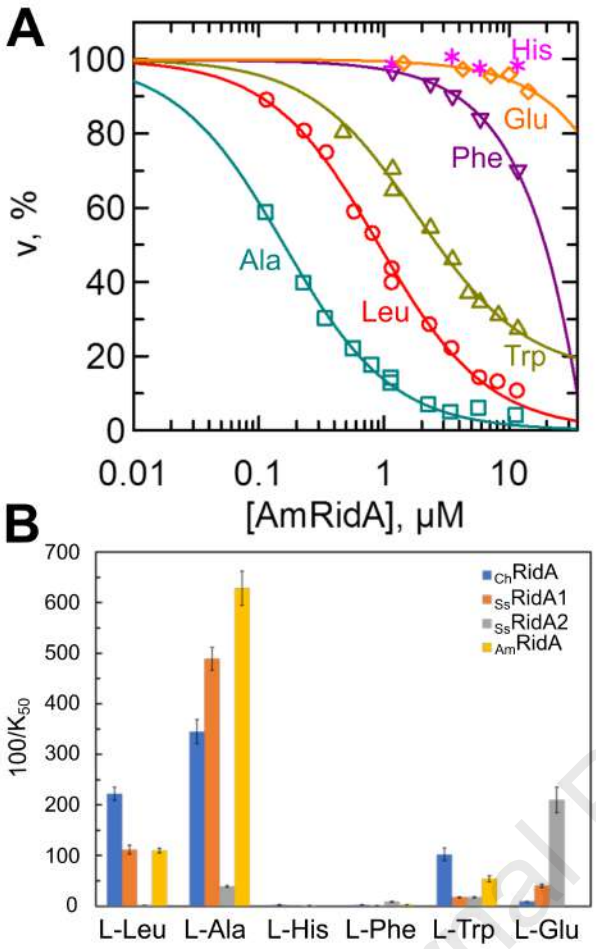

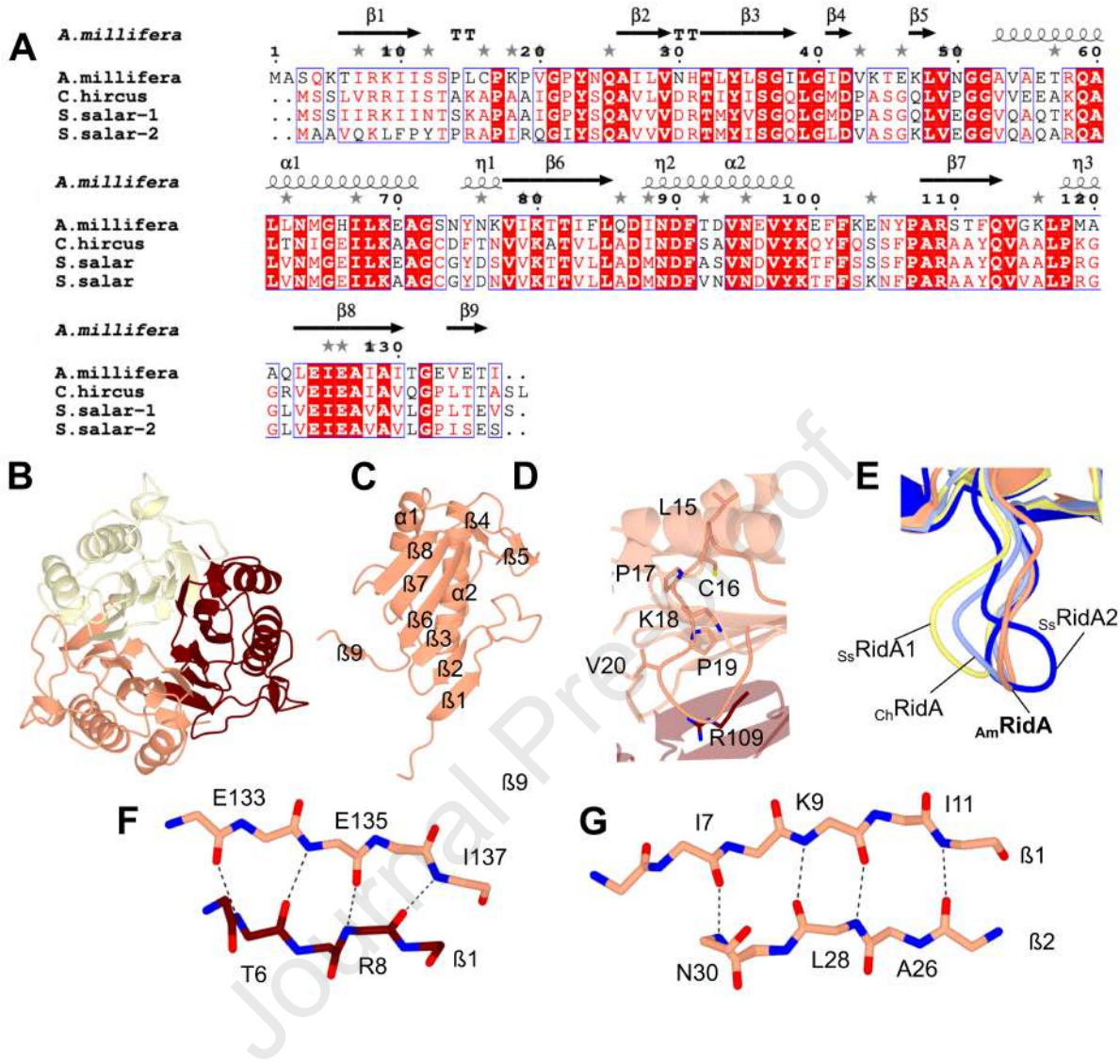

HIGHLIGHTS

- $_{Am}$RidA is the reactive intermediate deaminase from *Apis mellifera*.
- $_{Am}$RidA biochemical and structural properties resemble the ones of canonical RidAs.
- $_{Am}$RidA acts as deiminase.
- The crystal structure of $_{Am}$RidA was determined at 1.31 Å resolution.

Declaration of interests

☒ The authors declare that they have no known competing financial interests or personal relationships that could have appeared to influence the work reported in this paper.

☐ The authors declare the following financial interests/personal relationships which may be considered as potential competing interests: